Immunologic Profiling of Immune-Related Cutaneous Adverse Events with Checkpoint Inhibitors Reveals Polarized Actionable Pathways

Lacouture, Mario E ; Goleva, Elena ; Shah, Neil ; Rotemberg, Veronica ; Kraehenbuehl, Lukas ; Ketosugbo, Kwami F ; Merghoub, Taha ; Maier, Tara ; Bang, Alexander ; Gu, Stephanie ; Salvador, Trina ; Moy, Andrea P ; Lyubchenko, Taras ; Xiao, Olivia ; Hall, Clifton F ; Berdyshev, Evgeny ; Crooks, James ; Weight, Ryan ; Kern, Jeffrey A ; Leung, Donald Y M

DOI: https://doi.org/10.1158/1078-0432.ccr-23-3431

Immunologic Profiling of Immune-Related Cutaneous Adverse Events with Checkpoint Inhibitors Reveals Polarized Actionable Pathways

Mario E. Lacouture[1], Elena Goleva[2], Neil Shah[3], Veronica Rotemberg[1], Lukas Kraehenbuehl[1,4], Kwami F. Ketosugbo[1], Taha Merghoub[1,4], Tara Maier[1], Alexander Bang[1], Stephanie Gu[1], Trina Salvador[1], Andrea P. Moy[5], Taras Lyubchenko[2], Olivia Xiao[2], Clifton F. Hall[2], Evgeny Berdyshev[6], James Crooks[7], Ryan Weight[8], Jeffrey A. Kern[9], and Donald Y.M. Leung[2]

ABSTRACT

Purpose: Immune-related cutaneous adverse events (ircAE) occur in ≥50% of patients treated with checkpoint inhibitors, but the underlying mechanisms for ircAEs are poorly understood.

Experimental Design: Phenotyping/biomarker analyses were conducted in 200 patients on checkpoint inhibitors [139 with ircAEs and 61 without (control group)] to characterize their clinical presentation and immunologic endotypes. Cytokines were evaluated in skin biopsies, skin tape strip extracts, and plasma using real-time PCR and Meso Scale Discovery multiplex cytokine assays.

Results: Eight ircAE phenotypes were identified: pruritus (26%), maculopapular rash (MPR; 21%), eczema (19%), lichenoid (11%), urticaria (8%), psoriasiform (6%), vitiligo (5%), and bullous dermatitis (4%). All phenotypes showed skin lymphocyte and eosinophil infiltrates. Skin biopsy PCR revealed the highest increase in IFNγ mRNA in patients with lichenoid ($P < 0.0001$) and psoriasiform dermatitis ($P < 0.01$) as compared with patients without ircAEs, whereas the highest IL13 mRNA levels were detected in patients with eczema ($P < 0.0001$, compared with control). IL17A mRNA was selectively increased in psoriasiform ($P < 0.001$), lichenoid ($P < 0.0001$), bullous dermatitis ($P < 0.05$), and MPR ($P < 0.001$) compared with control. Distinct cytokine profiles were confirmed in skin tape strip and plasma. Analysis determined increased skin/plasma IL4 cytokine in pruritus, skin IL13 in eczema, plasma IL5 and IL31 in eczema and urticaria, and mixed-cytokine pathways in MPR. Broad inhibition via corticosteroids or type 2 cytokine–targeted inhibition resulted in clinical benefit in these ircAEs. In contrast, significant skin upregulation of type 1/type 17 pathways was found in psoriasiform, lichenoid, bullous dermatitis, and type 1 activation in vitiligo.

Conclusions: Distinct immunologic ircAE endotypes suggest actionable targets for precision medicine-based interventions.

Introduction

Checkpoint inhibitor (CPI) targeting programmed death 1 (PD1), programmed death ligand 1 (PDL1), and cytotoxic T-lymphocyte-associated protein 4 (CTLA4) receptors have been regulatory agency-approved as a monotherapy or in combination with cytotoxic chemotherapy or tyrosine kinase inhibitors for cancer treatment (1). Broad use of CPIs across solid and hematologic cancers in the neoadjuvant, adjuvant, and metastatic settings has improved clinical outcomes. Yet, their use is hampered by the development of all-grade adverse events (AE) in nearly 66% of patients, including ≥grade 3 AEs in up to 14% of patients (2–6). Among AEs, immune-related cutaneous adverse events (ircAE) are notable, given their high incidence [up to 26% grade 1 to 2 (7); 8% grade 3 to 4 (8)], chronicity (4)/delayed onset (9), and resistance/recurrence (10) with standard of care supportive interventions (11). These ircAEs are the first to present, some as early as 4 to 8 weeks since the initiation of therapy (10, 12); are usually persistent, with variable time to resolution (10); and may negatively impact the quality of life (QoL; refs. 13, 14) and therapeutic dose intensity (10, 15–18).

[1]Dermatology Service, Division of Subspecialty Medicine, Department of Medicine, Memorial Sloan Kettering Cancer Center, New York, New York. [2]Department of Pediatrics, National Jewish Health, Denver, Colorado. [3]Genitourinary Service, Department of Medicine, Memorial Sloan Kettering Cancer Center, New York, New York. [4]Ludwig Collaborative and Swim Across America Laboratory, Parker Institute for Cancer Immunotherapy, Human Oncology and Pathogenesis Program, Memorial Sloan Kettering Cancer Center, New York, New York. [5]Department of Pathology and Laboratory Medicine, Memorial Sloan Kettering Cancer Center, New York, New York. [6]Division of Pulmonary, Critical Care and Sleep Medicine, Department of Medicine, National Jewish Health, Denver, Colorado. [7]Division of Biostatistics and Bioinformatics, National Jewish Health, Denver, Colorado. [8]The Melanoma and Skin Cancer Institute, Denver, Colorado. [9]Division of Oncology, Department of Medicine, National Jewish Health, Denver, Colorado.

Current address for M.E. Lacouture: Dermatology Division, Department of Medicine, NYU Grossman Long Island School of Medicine, NYU Langone Hospital—Long Island, Mineola, New York; current address for L. Kraehenbuehl, Department of Dermatology, University Hospital Zurich USZ, University of Zurich UZH, Zurich, Switzerland; Department of Pharmacology and Meyer Cancer Center, Weill Cornell Medicine, New York, New York; and current address for T. Merghoub, Department of Pharmacology, Meyer Cancer Center, Weill Cornell Medicine, New York, New York.

M.E. Lacouture and E. Goleva co-first authors.

J.A. Kern and D.Y.M. Leung co-senior authors.

Corresponding Author: Elena Goleva, 1400 Jackson Street, Denver, CO 80206. E-mail: golevae@njhealth.org

Clin Cancer Res 2024;XX:XX–XX

doi: 10.1158/1078-0432.CCR-23-3431

Transitional Relevance

Deep phenotyping and biomarker analysis in checkpoint inhibitor–induced immune-related cutaneous adverse events (ircAE) revealed distinct immunologic pathways. Eight phenotypes exhibited unique circulating, histologic, and cytokine profiles, enabling targeted interventions. These findings suggest phenotype/endotype correlations are critical to understanding pathogenic mechanisms and refining therapeutic strategies in ircAEs.

To date, standard clinical practice and society guidelines recommend the use of histamine H1 receptor blockers, and topical/oral corticosteroids for ircAEs, which have limited efficacy for grade 2 to 3 ircAEs (15), are associated with additional toxicities, may impact the antitumor effects of CPIs (19), and are unsustainable for long-term use (20). Whereas various clinical presentations and histologic findings have been reported retrospectively, a prospective study has not been systematically conducted to assess outcomes (14) and define biomarkers (21) reflective of ircAE pathogenic mechanisms.

Hitherto, the mechanisms leading to CPI-induced ircAEs are poorly understood, although several hypotheses have been proposed, including reactivation of tissue-resident memory T cells (Trm; ref. 22), cross-reactivity between tumor- and self-antigens (23), breach of self-tolerance due to the removal of checkpoint blockade, tissue damage as a result of cytokine dysregulation, off-target effects in other organs that express immune checkpoint receptors targeted by CPI therapy (24), microbiome alterations (20), and tumor mutations (25). In this study, we combined clinical data with histopathology and comprehensive immune profiling in the skin and circulation to identify characteristic features of a large cohort of CPI-induced ircAEs. We hypothesized that ircAEs have specific immunologic pathways leading to varied clinical presentations, which may impact standard-of-care interventions. To overcome the limitations of previous reports, we studied 139 patients receiving CPIs presenting diverse ircAE phenotypes and compared them with 61 patients on CPIs with no ircAEs. Our primary objective was to define and correlate ircAE skin phenotypes with their immune reaction endotype and response to toxicity-directed therapy. We determined that specific immunologic endotypes were associated with the ircAE clinical phenotypes. These data also have identified targetable immune effectors that could mitigate these adverse events, ensure consistent CPI dosing, and improve patient QoL.

Materials and Methods

Study population

This open-label prospective, observational, multi-center study included a total of 200 patients who were on active treatment with CPI for cancer. Enrollment occurred at three sites, Memorial Sloan Kettering Cancer Center (MSK; New York, NY), National Jewish Health (Denver, CO), and The Melanoma and Skin Cancer Institute (Denver, CO), from April 2020 through the end of December 2022. Cohort 1 comprised 139 patients with ircAEs grade ≥2 per CTCAE version 5.0, whereas Cohort 2 (control group) comprised 61 patients who did not have an ircAE at the time of accrual. Inclusion criteria for both cohorts were as follows: age ≥18 years; diagnosis of a solid tumor; active treatment with US FDA–approved anti-PD1, anti-PDL1, or anti-CTLA4 therapies; and predicted life expectancy of ≥12 weeks. Patients were excluded from either cohort if they had received daily doses of systemic steroids in the previous 4 weeks for any indication other than treatment of an ircAE or as an antiemetic pre- or postchemotherapy; were enrolled in an investigational drug trial with a nonapproved therapy; were taking other CPIs beyond anti-PD1, anti-PDL1 or anti-CTLA4; had a current or previous diagnosis of leukemia or lymphoma; were pregnant; or had a known blood-borne infectious disease. The study was conducted in accordance with the ethical guidelines of the Declaration of Helsinki. The Institutional Review Boards of all participating institutions approved the study, and all participants gave signed informed consent prior to inclusion. This study was approved by the participating institutions' Institutional Review Boards (IRB #HS-3411) and was registered with the National Clinical Trials Network (NCTN04283539). The written informed consent was obtained from each study subject participant.

Study design

At the initial in-person visit, patients signed informed consent forms and providers collected information on their basic demographics (age, sex, race, and ethnicity), medical history, current medications, and any current AEs. Subjects then underwent a whole-body dermatologic exam and three-dimensional (3D) total body photography (3D TBP; Cohort 1 only; as described below). Standard of care hematologic and metabolic panel blood analysis was done for all study patients, and skin biopsy of selected lesional area for patients with ircAEs was collected. Research samples were obtained, including venous blood samples, skin tape stripping (STS; as described below), urine samples, and biopsied lesional skin tissues. Self-reported questionnaires were administered and included a standardized questionnaire about atopy/allergy family history and Skindex-16 questionnaire (26–30).

Although there may be overlap among certain ircAE phenotypes, we utilized American Academy of Dermatology criteria to classify phenotypes, such that eczema was clinically defined as pruritic, erythematous papules and plaques with serpiginous scaling and excoriations. Psoriasiform dermatitis featured sharply demarcated, erythematous plaques with a thick silvery scale most prominent over extensor surfaces including the elbows and knees. In contrast, lichenoid eruptions demonstrated violaceous, flat-topped polygonal papules that may coalesce into widespread plaques with an eczematous quality, often notable for significant pruritus.

Histologically, spongiosis and eosinophils typify eczematous dermatitis, whereas psoriasiform reactions exhibit parakeratosis, microabscesses with neutrophils, and hypogranulosis within an acanthotic epidermis. Conversely, lichenoid tissue responses present with a band-like lymphocytic infiltrate targeting the dermoepidermal junction.

Patients in Cohort 1 were prescribed treatments at the discretion of the consulting oncodermatologists in accordance with the phenotypic presentation of the rashes, had a second evaluation 4 to 6 weeks following enrollment, and underwent the same evaluations as at the initial baseline visit. Treatment decisions for ircAEs were made clinically based on the morphology, extent of involvement, and associated symptoms upon presentation, with laboratory data (i.e., absolute eosinophil count and serum IgE and IL6 levels) used as complementary information. Response to ircAE treatment was categorized as complete cutaneous response (CcR; reduction to CTCAE grade 0), partial cutaneous response (PcR; any reduction in CTCAE grade to grade ≥1), and cutaneous refractory (no change or clinical worsening).

Available clinical data related to diagnosis and staging were abstracted from the patients' electronic medical records, including pretreatment testing and tumor size, histologic subtype, and clinical stage at the time of enrollment based on criteria of the American Joint Committee on Cancer, eighth edition (31).

3D TBP

Patients in Cohort 1 underwent 3D TBP at their baseline and follow-up visits. 3D TBP was taken using the Vectra WB360 whole-body imaging system (Canfield Scientific, Parsippany, NJ), which uses 92 cameras to capture entire exposed body surfaces in a single capture. An assessor manually segmented surface area with visible rash on 3D TBP images using the program Vectra Analysis Module (VAM). This tool was previously used for quantitative assessment of cutaneous T-cell lymphoma involvement and calculation of the Modified Severity-Weighted Assessment Tool (12). All assessors were blinded to rash phenotype and in-person CTCAE grade. The percentage of the BSA with visible rash was calculated at each visit for each patient in Cohort 1.

Patient-reported outcomes

At every visit, patients completed a standardized Skindex-16 questionnaire, a 16-item patient-reported outcome (PRO) questionnaire defining the impact of skin-related conditions that occurred within the past week using a Likert scale (from 0 to 6, with 0 = never bothered and 6 = always bothered; ref. 26). Responses to the questions in the Skindex-16 are categorized into three subscales (domains): symptoms (four items), emotional (seven items), and functional (five items).

Histopathologic analysis

In this study, the diagnosis of each ircAE phenotype was established by clinical rash morphology. The histopathologic findings were used as complementary, and formal diagnosis was not made solely based on the histopathological data. Skin biopsies were obtained from all study patients in Cohorts 1 and 2. For Cohort 1, lesional skin biopsies from the rash site were assessed, whereas nonlesional skin biopsies were collected from patients in Cohort 2. Patients in Cohort 2 were given the option to opt out of skin biopsies. Skin biopsies were formalin-fixed, paraffin-embedded, processed for routine histologic examination with hematoxylin and eosin staining, and reviewed by a dermatopathologist, who was blinded to the patients' clinical group allocation. Histopathologic assessment of the skin biopsies included evaluation of the type and density of the inflammatory infiltrate. The density of tissue infiltration by lymphocytes, eosinophils, and neutrophils was graded as absent, present-mild, and present-moderate/severe. The density of lymphocytes was defined as moderate/severe if it was dense, confluent, and/or obscuring associated structures. Individual lymphocytes present in the skin biopsies were scored as present-mild. The density of eosinophils and neutrophils was defined as mild if <10 were identified in five consecutive high-power fields (HPF; magnification 200×) and moderate/severe if ≥10 per were identified in five HPFs. Skin biopsies were also taken for direct immunofluorescence (DIF) microscopy studies to assess antibodies and C3 complement component deposition. These studies were performed at an outside reference laboratory (Beutner Laboratories, Buffalo, NY) as per standard of care protocol and results were recorded based on reported findings.

Clinical laboratory peripheral blood assessment

Routine standard-of-care blood and chemistry analyses were abstracted from patients' medical records. The absolute and relative counts of peripheral venous blood lymphocytes, eosinophils, monocytes, neutrophils, basophils, and platelets were obtained. Blood serum samples were evaluated for IgE levels. The levels of anti-BP-180, anti-BP-230, anti-DSG-1, and anti-DSG-3 autoantibodies were determined in serum samples of Cohort 1 patients only.

Skin biopsy assessment via real-time PCR

Collected skin biopsies from Cohort 1 and Cohort 2 patients were submerged into TRI-reagent solution (Molecular Research Center Inc., Cincinnati, OH) for the RNA profiling. RNA was extracted following the manufacturer's protocol for the TRI-reagent preserved tissue samples. RNeasy Mini Kits (Qiagen, Hidden, Germany) were used to clean up the isolated RNA. Two hundred nanograms of the RNA samples were reverse-transcribed into complementary DNA using SuperScript VILO MasterMix according to the manufacturer's protocol (Life Technologies, ThermoFisher Scientific, Carlsbad, CA). Complementary DNA was analyzed via real-time PCR using an ABI QuantStudio 3 instrument (Applied Biosystems, ThermoFisher Scientific). Primers and probes for *18s RNA*, *IL13*, *IFNG*, and *IL17A* were purchased from Applied Biosystems, Thermo Fisher Scientific. The amounts of *IL13*, *IFNG*, and *IL17A* gene transcripts in skin biopsies were normalized to 18s RNA.

STS collection

Consecutive D-Squame tape strips (30 mm diameter, Clinical and Derm, Dallas, TX) were collected from the lesional skin of patients in Cohort 1 or from healthy skin areas of patients in Cohort 2. From each study patient, 20 STSs were obtained from each skin site studied. On application of the first tape disc, four marks were placed around the disc with a pen, so that subsequent discs could be applied to the same location. The collected tapes were stored on cardboard holders at −80°C until processing.

Cytokine multiplex assays

Collected plasma and STS samples were examined for the production of cytokines as described (32). Protein extracts were prepared from tape samples 9 and 10 of 20 STS that were collected. Tapes were sequentially submerged into Eppendorf tubes with PBS. Attached stratum corneum was removed from the adhesive side of the STS by agitation with 5 mm stainless steel beads (Qiagen) in TissueLyser (Qiagen) for 5 minutes at 25 Hz. After the procedure, STSs were removed from the buffer, and protein extracts were centrifuged for 10 minutes at 14,000 rpm to clear debris and adhesive residue. Samples were then concentrated using Sevant ISS110 Speed Vac Concentrator (ThermoScientific, Waltham, MA) and cryopreserved for future analysis. Total protein levels in STS extracts were measured with a detergent-compatible protein assay (Bio-Rad Laboratories, Hercules, California; RRID: SCR_008426). Protein extracts were analyzed according to the manufacturer's protocol with Meso Scale Discovery (MSD) U-Plex human cytokine multiplex platform on the MESO QuickPlex SQ 120MM Plate Reader (MSD, Rockville, MD; see Supplementary Table S1, key reagents). Preconfigured multiplex panels consisted of 20 analytes and included the analytes to profile levels of type 1 mediators [IFNγ-induced protein 10 kDa (IP)10, IL12 p70 subunit], type 2 mediators (IL4, IL5, IL13, and IL31), type 17/22 mediators (IL17A and IL22), regulatory cytokines (IL10), mediators of pro-inflammatory response (IL1a, IL6, IL8, IL18, TNFα, and IFNα2a), and chemokines and

alarmins [thymus and activation regulated chemokine (TARC), macrophage-derived chemokine (MDC), thymic stromal lymphopoietin (TSLP), IL33, and eotaxin]. Cytokine concentrations were calculated based on standard curves using the MSD Workbench Software with customized parameters. Cytokine concentrations below the fit curve range (signal below the bottom of the bottom-of-the-curve fit, no concentration given) were extrapolated below the standard curve detection limit. The remaining samples below detection were assigned half the value of the lowest detected sample concentration to maintain the ranking order. The MSD assay results for each STS-measured cytokine were normalized to the total protein amount in each STS sample and expressed as pg/mg protein. A total of 50 μL of plasma samples were allocated for analysis, and cytokine concentrations in plasma were expressed as pg/mL of plasma.

Statistical analysis

The *P* values for tests of differences between cohorts for distribution of demographic variables (age, gender, race, and ethnicity), cancer diagnosis variables (type and stage of cancer), cancer treatment variables (time on therapy, CPI class, and type of therapy) were calculated using a Wilcoxon rank sum test (age and time on therapy), Pearson's χ^2 test (gender), or Fisher's exact test with 5,000 replicates (race, ethnicity, type and stage of cancer, CPI class, and type of therapy). Values with $P < 0.05$ were considered statistically significant.

Clinical laboratory variables collected included concentrations of major cell types in the peripheral venous blood (eosinophils, basophils, neutrophils, platelets, lymphocytes, and monocytes) and serum IgE levels. Cytokine concentrations analyzed in MSD assays, serum IgE levels, and platelet counts were $\log_{10}$-transformed to normalize those variables. Differences in the medians of these variables between ircAE phenotypes and controls were calculated using robust quantile linear regression without covariate adjustment. The median quantile was estimated to ensure results were insensitive to extreme values. Standard errors were calculated using the bootstrap method with 100,000 replicates.

The amounts of cytokine transcripts in skin biopsies were compared using the Kruskal–Wallis nonparametric test with Dunn's multiple comparisons test.

Differences between responses from Cohort 1 and Cohort 2 participants on the Skindex-16 emotional subscale score, functional subscale score, symptom subscale score, and total scale were calculated using robust quantile linear regression without covariate adjustment. The median quantile was estimated to ensure results were insensitive to extreme values. Standard errors were calculated using the bootstrap method with 100,000 replicates. The same methodology was used for the analysis of differences between the cohorts for the median ($\log_{10}$-transformed) number of days on CPI therapy prior to study intake.

Data availability

Original data generated in the course of this study are available from the corresponding authors upon request. A structured public repository for the data generated in this manuscript does not exist.

Results

Patient demographics

Our overall study design is shown in **Fig. 1**. Two patient cohorts, both treated with CPIs, were accrued into this prospective, observational study: 139 with an ircAE (Cohort 1) and a control group of 61 patients with no ircAE (Cohort 2). As shown in Supplementary Table S2, both cohorts were balanced by age, sex, race, and ethnicity. Eight different ircAE phenotypes were identified in patients with an ircAE (Cohort 1): pruritus [$n = 36/139$ (25.9%)], maculopapular rash [MPR; $n = 30/139$ (21.6%)], eczema [$n = 26/139$ (18.7%)], lichenoid [$n = 15/139$ (10.8%)], urticaria [$n = 11/139$ (7.9%)], psoriasiform [$n = 9/139$ (6.5%)], vitiligo-like depigmentation [$n = 7/139$ (5.0%)], and bullous dermatitis [$n = 5/139$ (3.6%); **Table 1**]. Across ircAE phenotypes, age, gender, race, and ethnicity were comparable, except for the age of patients with bullous dermatitis, who were older (median age 85). The majority of patients examined in this study were White (80.5% of patients in the overall study cohort).

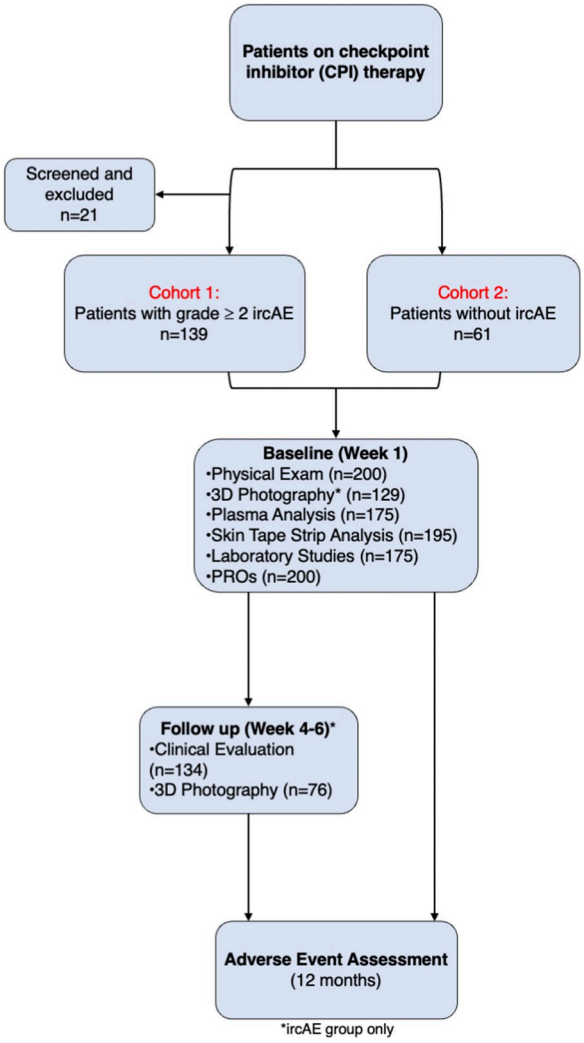

Figure 1.

Flow diagram of the evaluated cohorts and study accrual. Two patient cohorts, both treated with CPIs, were accrued into this prospective, observational study: 139 with an ircAE (Cohort 1) and a control group of 61 patients with no ircAE (Cohort 2). Patients were evaluated at baseline (week 1). Patients with ircAE have returned to a follow-up appointment 4 to 6 weeks later. All subjects underwent adverse events assessment 12 months after initial study enrollment. Evaluations performed at each visit are summarized in the flow diagram. ircAE, immune-related cutaneous adverse event; PRO, patient-reported outcomes.

Table 1. Demographics of study participants by ircAE phenotype.

Characteristic		Pruritus	Maculopapular rash	Eczema	Lichenoid dermatitis	Urticaria	Psoriasiform dermatitis	Vitiligo-like depigmentation	Bullous dermatitis
		$n = 36$	$n = 30$	$n = 26$	$n = 15$	$n = 11$	$n = 9$	$n = 7$	$n = 5$
Age (years)									
	Median	69 (56, 78)	63 (56, 70)	71 (65, 76)	67 (64, 76)	64 (57, 71)	69 (63, 78)	68 (48, 70)	85 (64, 89)
Gender									
	Female	14 (38.9)	12 (40.0)	9 (34.6)	10 (66.7)	5 (45.5)	2 (22.2)	5 (71.4)	1 (20.0)
	Male	22 (61.1)	18 (60.0)	17 (65.4)	5 (33.3)	6 (54.5)	7 (77.8)	2 (28.6)	4 (80.0)
Race									
	Asian	2 (5.6)	5 (16.7)	2 (7.7)	2 (13.3)	3 (27.3)	0 (0.0)	2 (28.6)	1 (20.0)
	Black or African American	1 (2.8)	1 (3.3)	2 (7.7)	0 (0.0)	1 (9.1)	0 (0.0)	3 (42.9)	0 (0.0)
	White	33 (91.7)	23 (76.7)	22 (84.6)	12 (80.0)	7 (63.6)	8 (88.9)	2 (28.6)	4 (80.0)
	More than one race	0 (0.0)	0 (0.0)	0 (0.0)	1 (6.7)	0 (0.0)	0 (0.0)	0 (0.0)	0 (0.0)
	Unknown/not reported	0 (0.0)	1 (3.3)	0 (0.0)	0 (0.0)	0 (0.0)	1 (11.1)	0 (0.0)	0 (0.0)
Ethnicity									
	Hispanic or Latino	5 (13.9)	1 (3.3)	2 (7.7)	0 (0.0)	0 (0.0)	1 (11.1)	1 (14.3)	0 (0.0)
	Not Hispanic or Latino	31 (86.1)	28 (93.3)	23 (88.5)	15 (100.0)	11 (100.0)	8 (88.9)	6 (85.7)	5 (100.0)
	Unknown/not reported	0 (0.0)	1 (3.3)	1 (3.8)	0 (0.0)	0 (0.0)	0 (0.0)	0 (0.0)	0 (0.0)

Values presented as median (interquartile range) for linear variables and number (percent) for categorical variables.

Cancer types and stages were similar between the ircAE and no ircAE cohorts (Supplementary Tables S3 and S4). The most frequent tumor types were renal, gastrointestinal, melanoma, and lung. All disease stages were represented in the study, with most patients with stage 4 disease (Supplementary Tables S3 and S4). PD1/PDL1 inhibition was the most frequent type of immunotherapy regimen (**Table 2**), and no significant difference between patients with ircAE versus those without ircAE was observed in terms of the agent type ($P = 0.3$; Supplementary Table S5). In a subset of patients (38.5% of patients in the overall cohort), CPI was combined with chemotherapy or targeted therapy, with no respective difference observed between the two cohorts (**Table 2**; Supplementary Table S5). When comparing between ircAE phenotypes, the CPI as monotherapy prevailed (**Table 2**). When comparing individual ircAE phenotypes, there was a difference in ircAEs depending on the CPI class used; the combination of CTLA4 and PD1/PDL1 inhibition was more commonly seen with MPR than other ircAEs (**Table 2**). No associations between the tumor type and the type of ircAE reaction were found in this study cohort (data not shown).

Patients with ircAEs had received CPI therapy for a median of 126 days (interquartile range 63 to 309), compared with patients without an ircAE (66 days, interquartile range 43 to 213) at the time of consent (Supplementary Table S5). The time to adverse event presentation differed significantly between the types of ircAE identified (**Table 2**). MPR developed the earliest, with a median time from CPI initiation and presentation of 38 days, whereas vitiligo-like depigmentation had the longest time from therapy to presentation, at a median of 443 days (**Table 2**). The standardized approach for patient characterization and specimen collection in this study is summarized in Supplementary Fig. S1.

3D TBP

Of the 139 patients in Cohort 1, 99 underwent 3D TBP at their baseline visit. The areas with visible cutaneous AEs on 3D TBP images were manually segmented for analysis. The distribution of body surface area (BSA) percentage affected in each phenotype is shown in **Fig. 2**. The area involved was the highest in the MPR group ($n = 30$) at 27.3% mean BSA and lowest in the pruritus group ($n = 30$) at 3.5%. By two-way analysis of variance (ANOVA) test ircAE by Common Terminology Criteria for Adverse Events (CTCAE) v5 at baseline ($P < 0.001$) and rash phenotype ($P = 0.002$) together were associated with the percentage of BSA affected by rash at baseline. Including all 159 TBP measurements between baseline and follow-up, by two-way ANOVA test, ircAE by CTCAE ($P < 0.001$) and phenotype ($P = 0.003$) together were associated with the percentage of body surface area affected by the AE.

PRO–QoL assessment

All study patients completed a standardized Skindex-16 questionnaire, a 16-item standardized PRO questionnaire defining the impact of skin-related conditions (26–30). Except vitiligo-like phenotype, a negative impact on QoL was reported across all ircAEs (**Fig. 2**), as defined by a higher total Skindex-16 scores ($0.0001 < P < 0.01$) when compared with Cohort 2. Similarly, the symptom ($0.0001 < P < 0.05$) and emotional ($0.0001 < P < 0.05$) domains were impacted in all ircAE phenotypes (except vitiligo-like depigmentation), when compared with Cohort 2 (**Fig. 2**). Conversely, only pruritus, MPR, and urticaria negatively affected patients' functional domain (e.g., showing affection, interaction with others, activities of daily living), ($0.001 < P < 0.05$, compared with Cohort 2; **Fig. 2**).

Clinical laboratory assessment of the peripheral blood samples

Clinical laboratory peripheral venous blood assessment determined that circulating total lymphocyte counts were decreased in pruritus ($P < 0.05$) and lichenoid phenotypes ($P < 0.01$). A trend for higher relative eosinophil counts was found in patients with

Table 2. CPI classes and therapeutic combinations received by study participants with ircAEs.

Characteristic		Pruritus *n* = 36	Maculopapular rash *n* = 30	Eczema *n* = 26	Lichenoid dermatitis *n* = 15	Urticaria *n* = 11	Psoriasiform dermatitis *n* = 9	Vitiligo-like depigmentation *n* = 7	Bullous dermatitis *n* = 5	*P* value[a]
Time on therapy (days)	216 (119, 345)	38 (16, 83)	224 (48, 448)	98 (60, 190)	154 (96, 406)	113 (72, 176)	443 (218, 963)	352 (300, 421)	<0.001	
CPI class										0.004
PD1/PDL1[b]		32 (88.9)	17 (56.7)	23 (88.5)	14 (93.3)	9 (81.8)	9 (100.0)	7 (100.0)	5 (100.0)	
PD1/PDL1 + CTLA4[c]	4 (11.1)	13 (43.3)	2 (7.7)	1 (6.7)	2 (18.2)	0 (0.0)	0 (0.0)	0 (0.0)		
PD1/PDL1 + Other[d]	0 (0.0)	0 (0.0)	1 (3.8)	0 (0.0)	0 (0.0)	0 (0.0)	0 (0.0)	0 (0.0)		
Type of therapy										0.093
CPI monotherapy		29 (80.5)	17 (56.7)	15 (57.7)	12 (80.0)	5 (45.5)	6 (66.7)	2 (29.0)	3 (60.0)	
CPI + Cytotoxic chemotherapy[e] ± Other[f]	3 (8.3)	4 (13.3)	4 (15.4)	1 (6.7)	3 (27.3)	1 (11.1)	0 (0.0)	0 (0.0)		
CPI + Kinase Inhibitor[g] ± Cytotoxic chemotherapy[e]	2 (5.6)	8 (26.7)	6 (23.1)	1 (6.7)	2 (18.2)	2 (22.2)	4 (57.0)	1 (20.0)		
CPI + Other[f]	2 (5.6)	1 (3.3)	1 (3.8)	1 (6.7)	1 (9.1)	0 (0.0)	1 (14.0)	1 (20.0)		

Values presented as median (interquartile range) for linear variables and number (percent) for categorical variables.
[a]Kruskal–Wallis rank sum test comparing time on therapy of each patient across all ircAEs; Fisher's exact test for count data with simulated *P* value (based on 5,000 replicates).
[b]Atezolizumab, dostarlimab, durvalumab, nivolumab, pembrolizumab.
[c]Ipilimumab, tremelimumab.
[d]Anti-TIGIT, T-cell immunoglobulin and immunoreceptor tyrosine-based inhibitory motif domain.
[e]Carboplatin, fluorouracil, gemcitabine, oxaloplatin, paclitaxel, pemetrexed, temozolomide.
[f]Abiraterone, denosumab, olaparib, rituximab, rucaparib, temsirolimus, tacrolimus.
[g]Axitinib, binimetinib, cabozantinib, encorafenib, entrectinib, levantinib, lucitanib, regorafenib, ruxolitinib, sitravatinib.

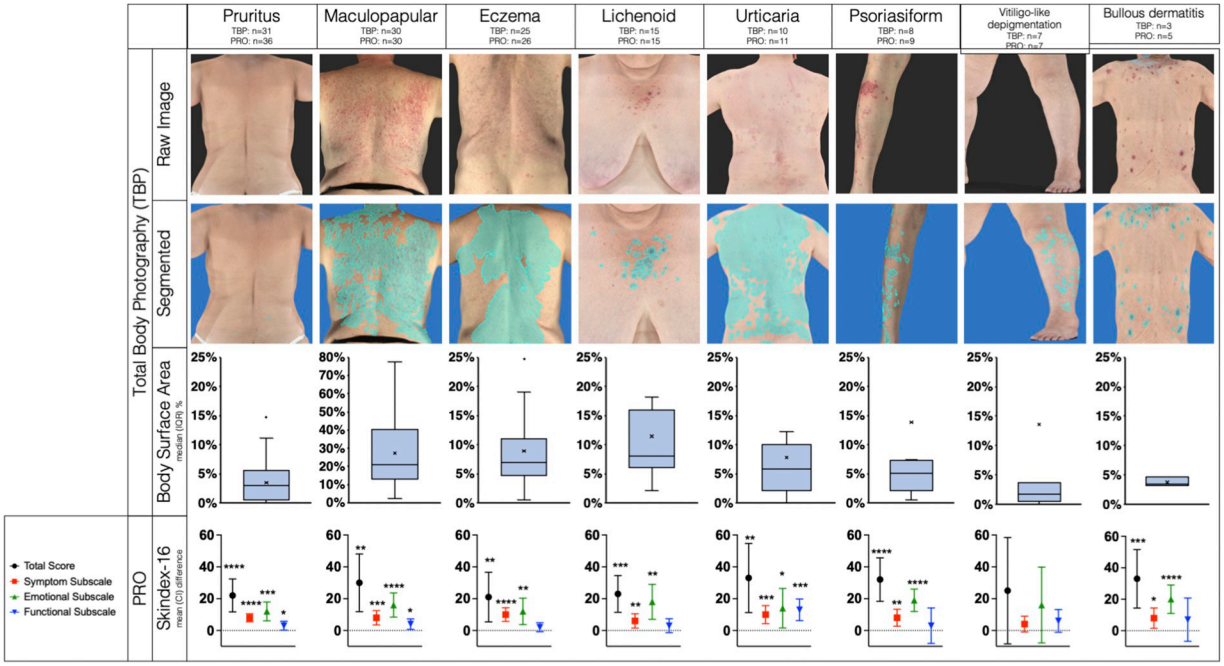

Figure 2.

ircAE phenotypes and patient-reported outcomes of skin symptoms. Representative images of the ircAEs as assessed by 3D total body photography with box and whisker plots of median (IQR, or interquartile range) of body surface area involvement of ircAE-related skin lesions as determined by segmentation using Vectra, and whisker plots of mean (CI, 95% confidence interval) difference of Skindex-16 domains (total, symptom, emotional, and functional) for patients with ircAEs (Cohort 1) when compared with control group (Cohort 2) are shown. *, $P < 0.05$; **, $P < 0.01$; ***, $P < 0.001$; ****, $P < 0.0001$.

eczematous rash (both $P = 0.06$; Supplementary Fig. S2). Median serum immunoglobin (Ig)E levels in Cohort 1 were not significantly different in comparison to Cohort 2 (Supplementary Fig. S3).

Serum samples of ircAE patients and Cohort 2 patients were tested for the presence of autoantibodies to desmoglein (DSG)-1, DSG-3 (33), and bullous pemphigoid (BP)-180 and BP-230 antigens (34), autoantibodies often associated with skin blistering diseases. Serum samples were considered positive if the levels of these antibodies were at least 20 relative units/ml or above. Circulating autoantibodies to BP-180 and BP-230 were detected in 3% and 9% ($n = 1$ of 34 and $n = 3$ of 34, respectively) of Cohort 2 patients tested, respectively. In comparison, these autoantibodies were detected in 9% and 2% ($n = 11$ of 125 and $n = 3$ of 125 patients) from the ircAE cohort. Among the ircAE cohort, anti-BP-180 antibodies were detected in 40% ($n = 2$ of 5 patients) of patients with bullous dermatitis, 31% ($n = 4$ out of 13) of patients with lichenoid rash, 13% ($n = 3$ of 24) of patients with eczema, 6% ($n = 2$ of 36) of patients with pruritus, and 4% ($n = 1$ of 26) of patients with MPR. Anti-BP-230 antibodies were present in 8% of lichenoid ($n = 1$ of 13), 4% of eczema ($n = 1$ of 24), and 3% of pruritus patients ($n = 1$ of 36). Anti-DSG-1 antibodies were detected in 13% ($n = 3$ of 24) of patients with eczema and 3% ($n = 1$ of 36) of patients with pruritus. Anti-DSG-3 antibodies were found in 8% ($n = 2$ out of 24) of patients with eczema and 4% ($n = 1$ of 26) of patients with MPR. Serum samples from two patients in Cohort 2, and two patients with eczema were positive for several autoantibodies.

Histopathology

In Cohort 2, lymphocytic infiltrates were absent in 91%, mild in 6%, and moderate/severe in 3%; eosinophilic and neutrophilic infiltrates were absent in 97% and mild in 3% of skin biopsies examined. In comparison with Cohort 2, histopathology of lesional skin from all ircAE clinical phenotypes showed significantly increased lymphocytic ($P < 0.0001$) and eosinophilic ($0.0001 < P < 0.05$) infiltrates (**Fig. 3**). Neutrophil density was increased among psoriasiform and urticarial skin phenotypes, as compared with controls ($P < 0.0001$, $P < 0.001$, respectively); there was no difference in neutrophilic infiltrate among lesional skin of other phenotypes.

DIF microscopy analysis detected deposition of antibodies (IgG, IgM, and IgA) and complement component C3 in subsets of ircAE patients (**Fig. 3**). Notably, linear deposition of IgG and C3 was identified in 60% ($n = 3$ of 5) and 80% ($n = 4$ of 5) of biopsies from patients that clinically presented with bullous dermatitis, respectively. Other patterns of staining observed at the dermo-epidermal junction included granular and globular staining, the significance of which is unclear. No intercellular antibody or complement deposition was detected within the epidermis. DIF assessment was not performed for Cohort 2 patients.

Skin and plasma biomarker profiling

Lesional skin biopsy samples from patients in Cohort 1 (ircAE group) and nonlesional skin biopsy samples from Cohort 2 patients were examined by targeted real-time PCR for the production of *IFNG*, *IL13*, and *IL17A* gene transcripts, to test whether ircAE phenotypes were associated with selectively polarized type 1 (IFNγ), type 2 (IL13), or type 17 (IL17A) inflammatory responses. As compared with skin biopsies from Cohort 2 (control patients on CPI without ircAE), a significant increase in *IFNG* mRNA levels was observed in the lesional skin of patients with lichenoid dermatitis

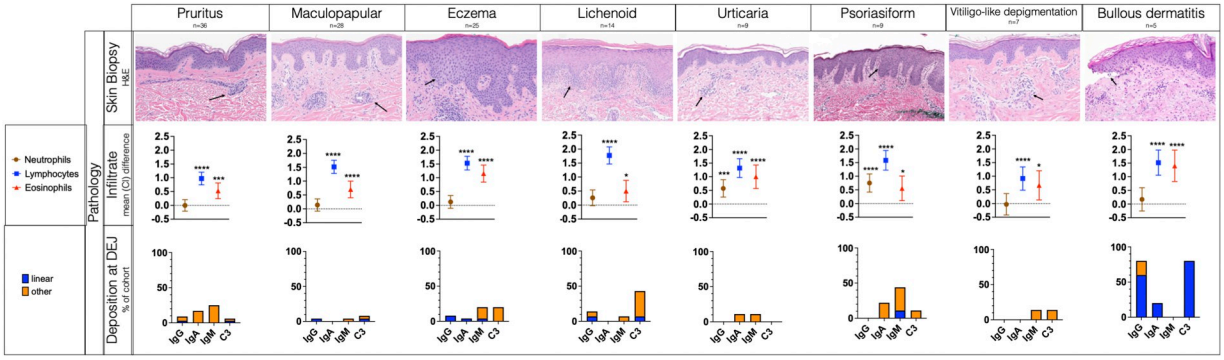

Figure 3.

Histological assessment of lesional skin biopsies of identified ircAE phenotypes. Representative images of lesional skin biopsy hematoxylin and eosin (H&E) staining, with whisker plot of the mean (CI, or 95% confidence interval) illustrating the difference of neutrophil, lymphocyte, and eosinophil infiltrate when compared with controls (*, $P < 0.05$; **, $P < 0.01$; ***, $P < 0.001$; ****, $P < 0.0001$). The summaries of DIF microscopy assessment of immunoglobin (Ig) and complement component 3 (C3) deposition at the dermoepidermal junction (DEJ) of skin biopsies are presented as bar graph plots showing the percentage of patients within each ircAE phenotype with linear or other (granular, globular, and other) antibody or C3 deposition at the DEJ. DIF analysis was performed for the ircAE cohort (Cohort 1) only.

($P < 0.0001$), psoriasiform dermatitis ($P < 0.01$), MPR ($P < 0.0001$), and eczema ($P < 0.01$), with the highest increase in *IFNG* mRNA levels observed in patients with lichenoid and psoriasiform dermatitis (46 and 18 median fold increase, respectively, as compared with Cohort 2), demonstrating type 1 inflammatory responses (**Fig. 4**). Significant increase in *IL13* mRNA levels was found in lesional skin of patients with eczema ($P < 0.0001$), bullous dermatitis ($P < 0.01$), lichenoid dermatitis ($P < 0.05$), and MPR ($P < 0.05$), as compared with Cohort 2 (**Fig. 4**). The highest amounts of *IL13* mRNA transcripts were detected in the eczema group (132 median fold increase as compared with Cohort 2), demonstrating a type 2 inflammatory response. Lastly, *IL17A* mRNA was found selectively increased in patients with psoriasiform ($P < 0.001$), lichenoid ($P < 0.0001$), and bullous dermatitis ($P < 0.05$) and MPR ($P < 0.001$) as compared with Cohort 2 (**Fig. 4**). *IL17A* mRNA levels were the highest in the psoriasiform dermatitis group (10^7 median fold increase as compared with Cohort 2, where it was rarely detected).

The utility of STSs and plasma profiling for the inflammatory mediators in the ircAE groups was also investigated. Distinct cytokine profiles were identified in STS and plasma samples from patients in Cohort 1 (**Fig. 5**), when compared with those from Cohort 2, illustrated as "0 line" in **Fig. 5**. Upon analysis, patients with pruritus had significant elevation in IL4 ($P < 0.01$) and IL12 p70 levels in the skin ($P < 0.05$), supporting type 2 cytokine activation and activation of IL12-producing dendritic cells/monocytes. Plasma samples from pruritus patients also provided evidence for the systemic activation of type 2 cytokine production [significant increase in the production of IL4 ($P < 0.0001$) and IL5 ($P < 0.01$)]. Increased levels of IL17a and decreased levels of IP10 (CXCL10; a type 1 inflammatory mediator) were also noted in plasma samples of patients with pruritus. Similarly, evidence for increased systemic type 2 cytokines production was also found in plasma samples of patients with eczema and urticaria, as shown by significantly increased levels of IL5 ($P < 0.0001$ and $P < 0.05$, respectively) and IL31 ($P < 0.05$). At the skin site, as defined by STS analysis, patients with eczema demonstrated a significant increase in the production of IP10. A nonpolarized immune response activation was found both at the skin lesions and in the circulation of patients with MPR, with

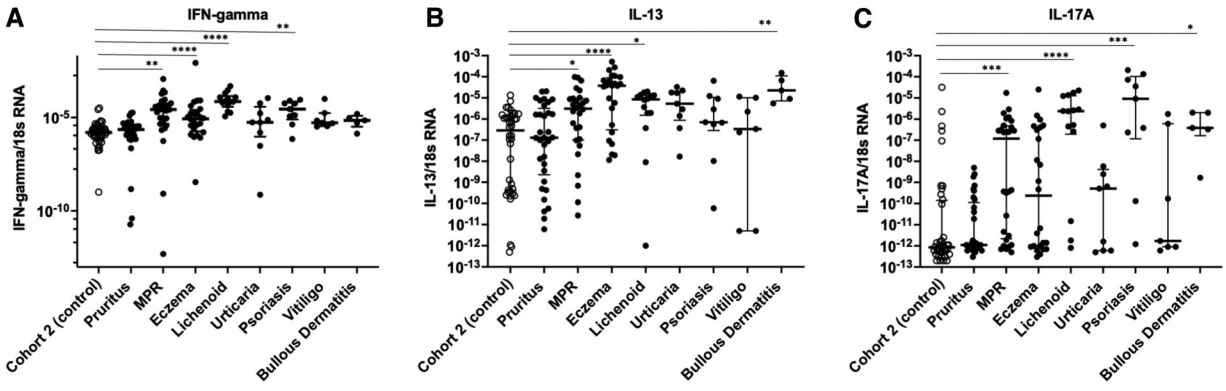

Figure 4.

IFNG, *IL13*, and *IL17A* transcripts in skin biopsy samples of patients with cancer experiencing checkpoint inhibitor–induced ircAEs. The expression of *IFNG* (**A**), *IL13* (**B**), and *IL17A* (**C**) mRNA was analyzed in lesional skin biopsies of patients with ircAEs and nonlesional skin biopsies of patients with no ircAEs. The data are presented as individual data points with median (interquartile range) for the corresponding ircAE type (Cohort 1) vs. control group with no ircAE (Cohort 2) on checkpoint inhibitor immunotherapy. *, $P < 0.05$; **, $P < 0.01$; ***, $P < 0.001$; ****, $P < 0.0001$.

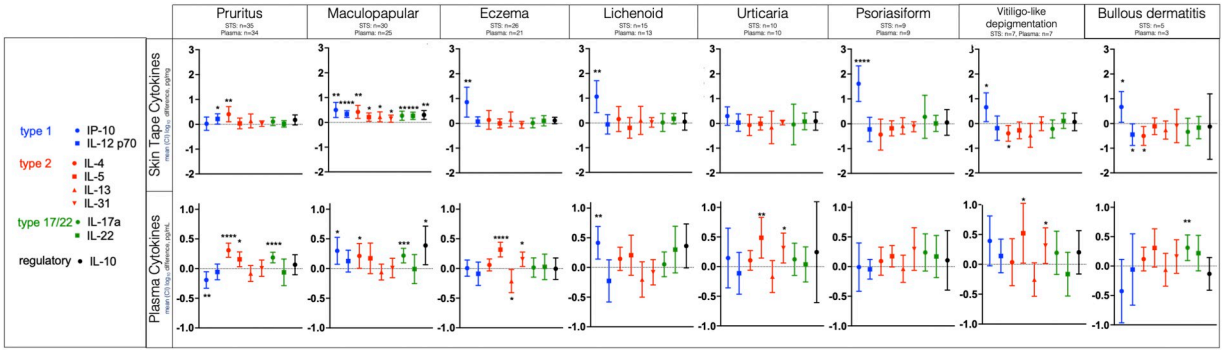

Figure 5.

Levels of type 1, type 2, type 17/22, and regulatory cytokines in the STS and plasma samples of patients with cancer experiencing checkpoint inhibitor–induced immune-related cutaneous adverse events (ircAEs). The data are presented as the whisker plots of the mean (CI, or 95% confidence interval) $\log_{10}$ difference in the cytokine concentration for the corresponding ircAE type (Cohort 1) vs. control group with no ircAE (Cohort 2) on checkpoint inhibitor immunotherapy (shown as the "0" line). The STS cytokine concentrations are measured in pg/mg protein; plasma cytokine concentrations are measured in pg/mL of plasma. *, $P < 0.05$; **, $P < 0.01$; ***, $P < 0.001$; ****, $P < 0.0001$.

a significant increase in production of type 1, type 2, type 17/22, and regulatory IL10 cytokines in the skin (as detected by STS analysis) and plasma, as compared with those in Cohort 2.

Patients with lichenoid, psoriasiform, vitiligo-like depigmentation, and bullous dermatitis demonstrated selective and significant upregulation of type 1 cytokine–regulated IP10 in the skin ($P < 0.01$) as compared with those in Cohort 2 (**Fig. 5**), as assessed by STS analysis. The most significant increase in the skin IP10 levels (nearly 30-fold, as compared with Cohort 2, $P < 0.0001$) was found in psoriasiform lesions. Systemically, significant upregulation of IP10 levels was only found in the plasma samples of patients with lichenoid rashes.

No significant changes in the production of type 1, type 2, and type 17/22 cytokines and IL10 were found in the plasma samples of patients with psoriasiform lesions as compared with those in Cohort 2 (**Fig. 5**). Significant increase in plasma IL17a levels was observed in the plasma samples of patients with bullous dermatitis ($P < 0.01$) as compared with those in Cohort 2. Increased levels of type 2 cytokines IL5 ($P < 0.05$) and IL31 ($P < 0.05$) were found in plasma samples of patients with vitiligo-like depigmentation as compared with Cohort 2. In addition, significant changes in the production of pro-inflammatory cytokines, chemokines, and alarmins were found in the skin and plasma samples of all patients in Cohort 1 (Supplementary Fig. S4).

Treatment responses

Of 139 patients in Cohort 1, 132 (95.0%) received supportive care interventions and had a follow-up visit to assess their response to therapy. Treatments were prescribed by oncodermatologists by the phenotypic presentation of the rashes. They included biologic agents ($n = 60$ of 132 patients evaluated, 45.5%), topical agents plus oral antipruritics ($n = 45$, 34.1%), topical agents alone ($n = 21$, 15.9%), and systemic steroids ($n = 10$, 7.6%). Biologics administered included dupilumab (anti-IL4 receptor; $n = 28$, 46.7%), omalizumab (anti-IgE; $n = 20$, 33.3%), benralizumab (anti-IL5; $n = 5$, 8.3%), ustekinumab (anti-IL12 p40 subunit; $n = 4$, 6.7%), and adalimumab (anti-TNFa), infliximab (anti-TNFa), and tocilizumab (anti-IL6 receptor; each $n = 1$, 1.7%).

Interventions set forth above resulted in a CcR in 35.3% of patients with pruritus ($n = 12$ of 34 patients available to follow up), 51.7% with MPR ($n = 15$ of 29 patients), 42.3% with eczema ($n = 11$ of 26), 21.4% with lichenoid rash ($n = 3$ of 14), 81.8% with urticaria ($n = 9$ of 11), 12.5% with psoriasiform ($n = 1$ of 8), and 40.0% with bullous dermatitis ($n = 2$ of 5) phenotypes (Supplementary Fig. S5). PcR was observed in 47.1% of patients with pruritus ($n = 16$ out of 34 patients available to follow up), 41.4% with MPR ($n = 12$ out of 29 patients), 50.0% with eczema ($n = 13$ out of 26), 71.4% with lichenoid rash ($n = 10$ out of 14), 18.2% with urticaria ($n = 2$ out of 11), 75.0% with psoriasiform rash ($n = 6$ out of 8), 16.7% with vitiligo-like depigmentation ($n = 1$ out of 5), and 40.0% with bullous dermatitis ($n = 2$ out of 5). Notably, systemic therapies resulted in CcR or PcR in the following settings: for pruritus, omalizumab ($n = 6$, 100%); for pruritus, dupilumab ($n = 7$, 100%); for MPR, benralizumab ($n = 2$, 40%); for eczema, dupilumab ($n = 14$, 87.5%); for urticaria, omalizumab ($n = 8$, 100%); for psoriasis, ustekinumab ($n = 3$, 100%); and for MPR, systemic steroids ($n = 6$, 100%; Supplementary Figs. S5 and S6). Representative clinical images of select ircAEs and response to therapy are presented in Supplementary Fig. S6; the cytokines targeted by selected biologics are illustrated in Supplementary Fig. S7.

Discussion

Our current study is the most extensive prospective, observational, multi-center study to characterize ircAEs in oncology patients on CPI. This NIAMS/NIH-funded study not only characterized the ircAE phenotypes and endotypes but also prospectively assessed the effects of treatment outcomes. Our findings confirmed that distinct ircAE phenotypes can be characterized clinically and through blood and skin biomarkers. These phenotypes have unique clinical patterns amenable to therapies targeting upregulated inflammatory pathways. Specifically, activation of type 2 immune responses was found in the skin and circulation of patients with ircAE pruritus, eczema, and urticaria, whereas the skin of patients with ircAE psoriasis, lichenoid and/or bullous dermatitis, and vitiligo-like depigmentation had significant activation of the mediators of type 1 and/or type 17 inflammation, characteristic of cytotoxic and autoimmune responses. Patients with MPR as an ircAE had nonpolarized immune activation, with the mediators of type 1, type 2, and type 17 inflammation detected in the skin and

circulation of these patients. Importantly, prospective use of biologics targeting type 2 inflammation [dupilumab, anti-IL4 receptor (IL4R); omalizumab, anti-IgE] in selected patients with eczema and pruritus demonstrated CcR or PcR in these patients, suggesting the importance of type 2–mediated pathways in the ircAE development in these patients. Likewise, limited use of anti-IL12p40 targeting antibody, ustekinumab, in patients with psoriasis phenotype provided a CcR or a PcR, signifying the contribution of type 1/type 17–mediated pathways in the formation of these psoriasiform ircAE lesions.

An increase in plasma IL5 levels in patients with ircAEs coexisted with eosinophils in lesional skin; a trend for higher levels of circulatory eosinophils was also identified in the blood of patients with eczematous ircAE. The effect of CPI on myeloid cells and the influence of myeloid cells on the CPI response has not been ascertained. However, a recent study documented that CPI treatment induced an increase in systemic IL5 production, driven by $CD4^+$ cells, which stimulated eosinophilopoiesis, resulting in systemic eosinophil accumulation (35). The study demonstrated that upon stimulation with anti-PD1, IL5 production was induced in peripheral blood $CD4^+$ T cells from patients with cancer, indicating that CPI can directly stimulate $CD4^+$ T cells to secrete IL5 (35), although to date it was not established whether IL5 production is a universal consequence of PD1 blockade in $CD4^+$ T cells. The study further showed that eosinophil expansion facilitated the recruitment of $CD8^+$ T cells to the tumor, promoting the production of chemoattractants for T cells and T cells' activation at the tumor site. The induction of IL33 was required to achieve intra-tumoral accumulation of eosinophils. Thus, eosinophils are accessory cells that can affect the response to cancer immunotherapy (36). On the other hand, abundant eosinophils within tumors may skew toward a Th2 endotype, abrogating the Th1 response, resulting in a tumor-promoting effect (37). Importantly, the role of PD1/PDL1 signaling in controlling IL5 secretion from $CD4^+$ T cells has been previously proposed in the context of allergy, when *in vitro* exposure of human allergen-specific $CD4^+$ T cells to PD1 blockade stimulated their production of IL5 among other cytokines (38). Further studies should focus on identifying the approaches that will allow fine-tuning of IL5 activation and eosinophilia during the CPI treatment, as these may not only influence antitumor response but may also be involved in ircAE development and tumor progression.

In our current study, a selective increase in IL4 production was found in the skin and circulation of patients with pruritus. IL4 is known to initiate type 2 inflammatory responses and is a critical cytokine that promotes IgE isotype switching. Both IL4 and IgE have been reported to promote and potentiate itch responses, activating peripheral neurons in the skin by engaging IL4R (39, 40) and causing the degranulation of mast cells and release of pruritogens triggered by IgE receptor crosslinking (40, 41). Both IL4R and IgE represent actionable targets that biologics can inhibit. In addition, the increased production of IL31, a type 2 cytokine and potent pruritogen, was found in CPI-induced eczema and urticaria. Anti-IL31 monoclonal antibodies have been recently shown to effectively inhibit itch responses (42).

A significant increase in *IL13* and *IFNG* mRNA was observed in patients with eczematous lesions. In addition, STS analysis revealed increased production of IP10, a type 1–regulated cytokine in the skin, along with type 2 cytokine activation in the circulation. In patients with atopic dermatitis, an inflammatory skin disease with prominent type 2 cytokine involvement, significantly increased levels of IP10 were also detected in the skin lesions and serum (43). A recent study using an animal model of atopic dermatitis demonstrated that IP10 production by keratinocytes regulated differentiation and activation of Th2 lymphocytes in the dermis (44). Our findings suggest that in the context of type 2 inflammatory response in ircAE eczema, an increase in skin IP10 may potentiate type 2 inflammation in the skin.

Of interest, the skin-specific and circulatory cytokine profile of patients with MPR demonstrated nonpolarized immune activation, as evidenced by significant increases of type 1, type 2, and type 17/22 cytokines at the skin rash site and in circulation. Moreover, an increase in the levels of the regulatory cytokine IL10 was found in their skin and plasma, likely a feedback response in an attempt to shut down the cytokine storm. IL10 is an anti-inflammatory cytokine that suppresses T-cell activation (45), and an increase in IL10 may inhibit T-cell activation. Given the nonpolarized immune activation in MPR ircAEs, the use of corticosteroids as a general anti-inflammatory treatment approach may be warranted in these patients.

It has been documented that CPI immunotherapy results in the activation of cytotoxic T-cell responses with the expansion of proliferating T-cell subsets and an increase in IFNγ-regulated proteins, which are strongly associated with the clinical response (46). MX1 (CXCL9) and IP10 (CXCL10) are produced by several cell types in response to IFNγ, regulating immune cell migration, differentiation, and activation (47), all of which are required for antitumor immune responses during CPI therapy (48). In this study, we found a significant increase in the production of IFNγ mRNA in the skin of patients with psoriasiform and lichenoid dermatitis, eczema, and MPR, with the highest amount detected in psoriasiform and lichenoid lesional skin sites. These data suggest that both antitumor responses and CPI-induced ircAEs could share common mediators, although the quantitative response may differ.

Beyond the activated T cells that respond to tumors, PD1 and other immune checkpoint receptors are also expressed by the differentiated T-cell subsets, including Trm, that are abundant in barrier organs such as the gastrointestinal tract and skin (22). Recent investigations of the cellular infiltrates in CPI-induced toxicities identified the expansion and activation of $CD8^+$ and $CD4^+$ Trm cells, suggesting that these cells became reactivated following CPI immunotherapy (49–51). Transcriptomic and immunostaining analysis determined predominant activation of IFNγ and cytolysins production by the activated Trm cells in irAE colitis and, recently, in irAE dermatitis, and provided evidence for the production of IFNγ activated targets (CXCL9, CXCL10, and CXCL11) by the myeloid and epithelial cells in the inflamed tissues (49–51).

Luoma and colleagues (49) performed single-cell analysis of immune cell populations in irAE colitis and reported accumulation of $CD8^+$ T cells with highly cytotoxic and proliferative states and no T regulatory cell depletion in the inflamed colon. T-cell receptor sequence analysis demonstrated that the majority of activated $CD8^+$ T cells originated from Trm populations. These cells were shown to express high levels of CPI receptors and integrins. It was suggested that CXCL9-11 produced by myeloid and epithelial cells participated in the recruitment of additional T cells into the intestinal tissue, facilitating the inflammatory response. In an independent study, Sasson and colleagues (50) confirmed that $CD8^+$ Trm cells are the dominant activated T-cell subset in both anti-CTLA4/PD1 combination therapy and anti-PD1 inhibitor–associated colitis. Activation of these cells was found to correlate with clinical and endoscopic colitis severity. Recently, Reschke and colleagues (51) using multiparameter tissue immunostaining, spatial transcriptomics, and RNA *in situ* hybridization determined that $CD4^+$

and $CD8^+$ Trm cells were expanded in ircAE dermatitis, expression of IFNγ, CXCL9, CXCL10, and TNF-alpha was found in the lesional skin, with IFNγ specifically expressed by Trm cells. The Th1-skewed phenotype was also confirmed in irAE colitis cases compared with a healthy colon. Goldinger and colleagues (52) examined CPI-induced dermatitis in patients with melanoma. Twenty-two percent of patients developed cutaneous reactions, and 15% developed vitiligo. The cutaneous reactions ranged from erythematous papules with mild pruritus to disseminated erythematous MPR without signs of epidermal involvement to severe MPRs, including epidermal detachment and mucosal involvement. The study described a patient who initially developed an MPR reaction to CPI treatment; skin tissue immunostaining analysis from this patient revealed an accumulation of $CD8^+$ cells at the dermoepidermal junction and keratinocyte apoptosis. Despite the systemic treatment with corticosteroids, the lesional skin of this patient evolved into lichen planus. Gene expression analysis of lesional skin samples from anti-PD1-treated patients revealed a gene expression profile resembling Stevens-Johnson syndrome/toxic epidermal necrolysis with an upregulation of CXCL9, CXCL10, and CXCL11, granzymes, pro-apoptotic molecules, and CPI receptors. The cytokine findings in our study also support the reactivation of skin Trm cells but suggest that the cytokine profile produced by these cells could be polarized and rash-specific.

In addition, in our study, STS analysis revealed that IFNγ inducible IP10 was significantly elevated in patients with psoriasiform, lichenoid, bullous dermatitis, eczema, and vitiligo-like depigmentation, with the highest increase noted in psoriasiform ircAEs. Conversely, IP10 was increased in the plasma of lichenoid ircAEs only. Importantly, a recent study demonstrated that detection of proliferating T-cell subsets at 1 to 2 weeks after the start of CPI therapy can help identify those patients at higher risk of CPI toxicity; specifically, increased CXCL9 and IP10 (CXCL10) and reduced IL10 shortly after the start of CPI therapy in melanoma and non-small cell lung carcinoma were shown to be likely indicators of heightened risk of developing any irAE, including ircAEs (53). The increase in plasma proteins that are associated with the IFNγ signaling pathway in patients with irAEs may be linked to the expansion of Ki-67 $CD8^+$ T cells, which express the CXCL9/CXCL10 receptor, CXCR3 (46). Prominent activation of type 1 immune response in several skin ircAE types suggests that topical JAK inhibitors should be considered to dial down the inflammation at the skin site (54). In addition, selective increase in *IL17A* mRNA levels in skin biopsies of patients with psoriasiform, lichenoid, and bullous dermatitis may suggest the contribution of IL17-driven autoimmune responses in these ircAEs. Thus, targeted inhibition of type 17 inflammation with biologic agents could also be considered for these ircAEs.

Overall, these findings show that the combined assessment of skin and systemic cytokines in ircAEs provides a robust assessment tool for phenotyping and suggests targeted lines of therapy for symptom alleviation. As skin toxicities associated with CPI immunotherapy are often associated with tumor responsiveness, if ircAEs occur, the primary goal should be to improve patient care through effective monitoring and timely rash intervention. The identified rash-specific biomarkers, thus, provide effective rash management strategies and will allow patients to continue CPI immunotherapy (14).

The autoantibodies to BP antigens are an established feature of bullous pemphigoid and lichen planus pemphigoides (33, 34). The frequency of autoantibodies in other inflammatory skin rashes is not well established, but IgE autoantibodies to epithelial antigens have been frequently reported in moderate-to-severe atopic dermatitis patients (55, 56), whereas autoantibodies to cathelicidin and ADAMTSL5 have been detected in 20% to 30% patients with psoriatic arthritis, and to a lesser degree in psoriasis patients (57). Our study revealed the presence of autoantibodies to DSG-1, DSG-3, BP-180, and BP-230 in serum samples from a subset of patients from the ircAE cohort and some patients from Cohort 2 (no rash). The pathogenic role of these findings requires further investigation in conjunction with tissue DIF analysis. Although antibody and C3 deposition was seen at the dermoepidermal junction in a subset of tissue samples from ircAE patients, identification of the epidermal proteins targeted by these antibodies requires additional evaluation. Furthermore, several nonbullous dermatitis ircAE cases showed serum antibody positivity to the common blistering disease epidermal antigens, but these cases were not associated with the corresponding characteristic DIF findings. Of note, preclinical BP antibodies have been reported in aging patients with pruritus, neurological diseases, diabetes mellitus, and rheumatologic collagen diseases (58). Anti-DSG-1 and DSG-3 antibodies, along with other epidermal protein autoantibodies, have been found in paraneoplastic pemphigus and other autoimmune conditions (33). Additionally, the diagnostic value and clinical significance of nonlinear antibody and C3 deposition at the dermoepidermal junction in some cases (including granular and globular staining) is unclear.

Participants with ircAEs in our study were responsive to a combination of pharmacologic and/or biologic treatments, with 87.9% of patients ($n = 116$ of 132 ircAE patients that received treatment and were followed at the return visit) experiencing clinical improvement or resolution of their rash. Treatment with topical therapies and oral antipruritics showed modest benefits, which is consistent with what has been reported in the literature (10). Our study reports one of the largest cohorts of patients to date who received targeted biologic agents for the treatment of ircAEs. Across all ircAE phenotypes, a total of 91.7% ($n = 55$ of 60) of patients who were treated with biologics experienced clinical improvement. In addition, biologic agents provided a corticosteroid-sparing alternative, which is particularly important in these patients, as systemic steroids have been associated with toxicities in >90% of patients and may undermine the antitumor efficacy of CPIs (5). Although the therapies selected and subsequent responses elucidated herein aim to characterize empiric treatment considerations for ircAEs, the lack of a comparison control group precludes definitive conclusions regarding superiority amongst modalities. Indeed, treatment algorithms relied principally on clinical expertise regarding the predominant phenotypic features of the ircAE in question.

Study limitations

This study had several limitations. This was a cross-sectional study by design and patients on CPI with ircAE were only evaluated at the time of ircAE development. Hence, the information about the laboratory and clinical parameters for these patients prior to toxicity development was not available, to determine whether these patients were predisposed for the development of ircAEs. To do so would require longitudinal monitoring of patients prior to the start of CPI immunotherapy.

A second limitation was the relatively low patient number in some of the patient ircAE subgroups (vitiligo-like depigmentation, bullous dermatitis), this is mainly due to the real-world infrequency of these CPI-induced ircAE types. Overall, the two study cohorts were well balanced based on the cancer types, although, a somewhat higher proportion of patients with gastrointestinal cancers were enrolled in Cohort 1, whereas a greater proportion of patients with

melanomas was enrolled in Cohort 2; this was mainly driven by the oncology clinics specialties that were involved in enrollment of patients into these cohorts. All clinical stages were represented in both cohorts, with cancer stages significantly weighted toward advanced disease stages as expected, in accordance with the treatment guidelines. Though there were differences noted in stage and cancer type between groups, these differences should not bias the results as the focus on CPI-induced cutaneous events should be cancer type and stage independent.

Third, given that the median time on therapy in Control Cohort 2 was 66 days, whereas the median time of ircAE onset in Cohort 1 was 126 days, it is possible that some patients in Cohort 2 will also develop ircAE events in the future and therefore cannot be considered as a true control.

Fourth, in this study rash appearance was used to guide therapeutic decisions. The treatment findings reported in this study were meant to be descriptive, as we did not have a comparator group managed by an alternative treatment protocol, limiting conclusions about comparative treatment effectiveness from this dataset alone.

In summary, the current study is the largest prospective observational study of CPI-induced ircAEs; the study findings shed light on the pathobiological mechanisms of ircAEs, suggesting selective activation of type 2, type 1, and/or type 17 cytokines in specific ircAE types and identified rash-specific biomarkers that may help to monitor and treat patients with these toxicities using targeted biologics. Our study also determined that both peripheral blood and skin site cytokine analysis were required to provide a complete immunologic picture for the characterization of the ircAE endotypes. Beyond skin biopsy assessment, the study also demonstrated the utility of STS analysis for inflammatory cytokine profiling of the ircAE endotypes.

Authors' Disclosures

M.E. Lacouture reports grants and personal fees from Rubedo, onQuality, and Kintara as well as grants from AZ, Novartis, and Novocure outside the submitted work. E. Goleva reports grants from Sanofi/Genzyme outside the submitted work. N. Shah reports personal fees from Merck and Aveo and other support from Exelixis and Aravive, as well as personal fees from MJH and MedNet during the conduct of the study. V. Rotemberg reports grants from NIH/NCI during the conduct of the study as well as other support from Excite International and Inhabit Brands outside the submitted work. L. Kraehenbuehl reports grants from the Swiss National Science Foundation during the conduct of the study as well as personal fees from Janssen outside the submitted work. T. Merghoub reports a consultantship with Daiichi Sankyo Co, Leap Therapeutics, Immunos Therapeutics, and Pfizer and is co-founder of Imvaq Therapeutics. T. Merghoub has equity in Imvaq Therapeutics and reports grants from Bristol Myers Squibb, Realta, and Enterome. T. Merghoub is an inventor of patent applications related to work on oncolytic viral therapy, alphavirus-based vaccines, neo-antigen modeling, CD40, GITR, OX40, PD1, and CTLA4. A.P. Moy reports grants from NIH/NIAMS during the conduct of the study. E. Berdyshev reports grants from NIH during the conduct of the study. J. Crooks reports grants from NIH during the conduct of the study. R. Weight reports grants from NIH during the conduct of the study as well as personal fees from Merck, Immunocore, and Castle Biosciences outside the submitted work. J.A. Kern reports grants from NIAMS during the conduct of the study as well as other support from Cireca, LLC, outside the submitted work. No disclosures were reported by the other authors.

Authors' Contributions

M.E. Lacouture: Conceptualization, methodology, investigation, formal analysis, writing-original draft, writing-review and editing. **E. Goleva:** Conceptualization, methodology, investigation, formal analysis, writing-original draft, writing-review and editing. **N. Shah:** Resources, data curation, formal analysis, writing-review and editing. **V. Rotemberg:** Data curation, formal analysis, writing-review and editing. **L. Kraehenbuehl:** Resources, data curation, formal analysis, writing-review and editing. **K.F. Ketosugbo:** Resources, data curation, formal analysis, writing-review and editing. **T. Merghoub:** Resources, data curation, formal analysis, writing-review and editing. **T. Maier:** Resources, data curation, formal analysis, writing-review and editing. **A. Bang:**Resources, data curation, formal analysis, writing-review and editing. **S. Gu:** Resources, data curation, formal analysis, writing-review and editing. **T. Salvador:** Data curation, formal analysis, writing-review and editing. **A.P. Moy:** Data curation, formal analysis, writing-review and editing. **T. Lyubchenko:** Data curation, formal analysis, writing-review and editing. **O. Xiao:** Data curation, formal analysis, writing-review and editing. **C.F. Hall:** Data curation, writing-original draft, writing-review and editing. **E. Berdyshev:** Formal analysis, writing-review and editing. **J. Crooks:** Methodology, validation, writing-review and editing. **R. Weight:** Data curation, writing-review and editing. **J.A. Kern:** Conceptualization, methodology, investigation, formal analysis, writing-original draft, writing-review and editing. **D.Y. Leung:** Conceptualization, methodology, investigation, formal analysis, writing-original draft, writing-review and editing.

Acknowledgments

This project was supported by an NIH/NIAMS Grant (U01 AR077511) and an NIH/NCI Cancer Center Support Grant (P30 CA008748). L. Kraehenbuehl's research was also supported by a Swiss National Science Foundation Grant (P400PM_199318). Editorial support at Memorial Sloan Kettering Cancer Center was provided by Katharine Olla Inoue, MA.

Note

Supplementary data for this article are available at Clinical Cancer Research Online (http://clincancerres.aacrjournals.org/).

Received November 3, 2023; revised January 29, 2024; accepted April 19, 2024; published first April 23, 2024.

References

1. Vaddepally RK, Kharel P, Pandey R, Garje R, Chandra AB. Review of indications of FDA-approved immune checkpoint inhibitors per NCCN guidelines with the level of evidence. Cancers (Basel) 2020;12:738.
2. Thompson LL, Krasnow NA, Chang MS, Yoon J, Li EB, Polyakov NJ, et al. Patterns of cutaneous and noncutaneous immune-related adverse events among patients with advanced cancer. JAMA Dermatol 2021; 157:577–82.
3. Wang Y, Zhou S, Yang F, Qi X, Wang X, Guan X, et al. Treatment-related adverse events of PD-1 and PD-L1 inhibitors in clinical trials: a systematic review and meta-analysis. JAMA Oncol 2019;5:1008–19.
4. Naidoo J, Page DB, Li BT, Connell LC, Schindler K, Lacouture ME, et al. Toxicities of the anti-PD-1 and anti-PD-L1 immune checkpoint antibodies. Ann Oncol 2015;26:2375–91.
5. Das S, Johnson DB. Immune-related adverse events and anti-tumor efficacy of immune checkpoint inhibitors. J Immunother Cancer 2019;7:306.
6. Schneider BJ, Naidoo J, Santomasso BD, Lacchetti C, Adkins S, Anadkat M, et al. Management of immune-related adverse events in patients treated with immune checkpoint inhibitor therapy: ASCO guideline update. J Clin Oncol 2021;39:4073–126.
7. Belum VR, Benhuri B, Postow MA, Hellmann MD, Lesokhin AM, Segal NH, et al. Characterisation and management of dermatologic adverse events to agents targeting the PD-1 receptor. Eur J Cancer 2016;60:12–25.
8. Wang E, Kraehenbuehl L, Ketosugbo K, Kern JA, Lacouture ME, Leung DYM. Immune-related cutaneous adverse events due to checkpoint inhibitors. Ann Allergy Asthma Immunol 2021;126:613–22.
9. Jacoby TV, Asdourian MS, Shah N, Otto TS, Thompson LL, Reynolds KL, et al. Low grade cutaneous immune related adverse events leading to immunotherapy discontinuation. Clin Exp Dermatol 2023;48:1058–60.
10. Phillips GS, Wu J, Hellmann MD, Postow MA, Rizvi NA, Freites-Martinez A, et al. Treatment outcomes of immune-related cutaneous adverse events. J Clin Oncol 2019;37:2746–58.

11. Park BC, Jung S, Chen ST, Dewan AK, Johnson DB. Challenging dermatologic considerations associated with immune checkpoint inhibitors. Am J Clin Dermatol 2022;23:707–17.
12. Martins F, Sofiya L, Sykiotis GP, Lamine F, Maillard M, Fraga M, et al. Adverse effects of immune-checkpoint inhibitors: epidemiology, management and surveillance. Nat Rev Clin Oncol 2019;16:563–80.
13. Tattersall IW, Leventhal JS. Cutaneous toxicities of immune checkpoint inhibitors: the role of the dermatologist. Yale J Biol Med 2020;93:123–32.
14. Walocko FM, Ly BC, White MS, Chen SC, Yeung H. Health-related quality of life measures and immune checkpoint inhibitors: a systematic review. J Am Acad Dermatol 2020;82:1004–6.
15. Tomsitz D, Ruf T, Zierold S, French LE, Heinzerling L. Steroid-refractory immune-related adverse events induced by checkpoint inhibitors. Cancers (Basel) 2023;15:2538.
16. Verheijden RJ, van Eijs MJM, May AM, van Wijk F, Suijkerbuijk KPM. Immunosuppression for immune-related adverse events during checkpoint inhibition: an intricate balance. NPJ Precis Oncol 2023;7:41.
17. Brahmer JR, Abu-Sbeih H, Ascierto PA, Brufsky J, Cappelli LC, Cortazar FB, et al. Society for Immunotherapy of Cancer (SITC) clinical practice guideline on immune checkpoint inhibitor-related adverse events. J Immunother Cancer 2021;9:e002435.
18. Malkhasyan KA, Zakharia Y, Milhem M. Quality-of-life outcomes in patients with advanced melanoma: a review of the literature. Pigment Cell Melanoma Res 2017;30:511–20.
19. Mouri A, Kaira K, Yamaguchi O, Hashimoto K, Miura Y, Shiono A, et al. Effect of systemic steroid use for immune-related adverse events in patients with non-small cell lung cancer receiving PD-1 blockade drugs. J Clin Med 2021;10:3744.
20. Ramos-Casals M, Brahmer JR, Callahan MK, Flores-Chavez A, Keegan N, Khamashta MA, et al. Immune-related adverse events of checkpoint inhibitors. Nat Rev Dis Primers 2020;6:38.
21. Seervai RNH, Sinha A, Kulkarni RP. Mechanisms of dermatological toxicities to immune checkpoint inhibitor cancer therapies. Clin Exp Dermatol 2022;47:1928–42.
22. Dougan M, Luoma AM, Dougan SK, Wucherpfennig KW. Understanding and treating the inflammatory adverse events of cancer immunotherapy. Cell 2021;184:1575–88.
23. Berner F, Bomze D, Diem S, Ali OH, Fassler M, Ring S, et al. Association of checkpoint inhibitor-induced toxic effects with shared cancer and tissue antigens in non-small cell lung cancer. JAMA Oncol 2019;5:1043–7.
24. Esfahani K, Elkrief A, Calabrese C, Lapointe R, Hudson M, Routy B, et al. Moving towards personalized treatments of immune-related adverse events. Nat Rev Clin Oncol 2020;17:504–15.
25. Bomze D, Hasan Ali O, Bate A, Flatz L. Association between immune-related adverse events during anti-PD-1 therapy and tumor mutational burden. JAMA Oncol 2019;5:1633–5.
26. Atherton PJ, Burger KN, Loprinzi CL, Neben Wittich MA, Miller RC, Jatoi A, et al. Using the Skindex-16 and common terminology criteria for adverse events to assess rash symptoms: results of a pooled-analysis (N0993). Support Care Cancer 2012;20:1729–35.
27. Chren MM, Lasek RJ, Sahay AP, Sands LP. Measurement properties of Skindex-16: a brief quality-of-life measure for patients with skin diseases. J Cutan Med Surg 2001;5:105–10.
28. Chren MM, Lasek RJ, Quinn LM, Mostow EN, Zyzanski SJ. Skindex, a quality-of-life measure for patients with skin disease: reliability, validity, and responsiveness. J Invest Dermatol 1996;107:707–13.
29. Chren MM, Lasek RJ, Quinn LM, Covinsky KE. Convergent and discriminant validity of a generic and a disease-specific instrument to measure quality of life in patients with skin disease. J Invest Dermatol 1997;108:103–7.
30. Chren MM, Lasek RJ, Flocke SA, Zyzanski SJ. Improved discriminative and evaluative capability of a refined version of Skindex, a quality-of-life instrument for patients with skin diseases. Arch Dermatol 1997;133:1433–40.
31. Amin M, Edge S, Greene F, Byrd D, Brookland R, Washington M, et al. American Joint Committee on Cancer (AJCC) cancer staging manual, 8th ed Springer International Publishing: American Joint Commission on Cancer; 2017.
32. Lyubchenko T, Collins HK, Goleva E, Leung DYM. Skin tape sampling technique identifies proinflammatory cytokines in atopic dermatitis skin. Ann Allergy Asthma Immunol 2021;126:46–53.e2.
33. Schmidt E, Kasperkiewicz M, Joly P. Pemphigus. Lancet 2019;394:882–94.
34. Bagci IS, Horvath ON, Ruzicka T, Sardy M. Bullous pemphigoid. Autoimmun Rev 2017;16:445–55.
35. Blomberg OS, Spagnuolo L, Garner H, Voorwerk L, Isaeva OI, van Dyk E, et al. IL-5-producing $CD4^+$ T cells and eosinophils cooperate to enhance response to immune checkpoint blockade in breast cancer. Cancer Cell 2023;41:106–23.e10.
36. Grisaru-Tal S, Rothenberg ME, Munitz A. Eosinophil-lymphocyte interactions in the tumor microenvironment and cancer immunotherapy. Nat Immunol 2022;23:1309–16.
37. Ikutani M, Yanagibashi T, Ogasawara M, Tsuneyama K, Yamamoto S, Hattori Y, et al. Identification of innate IL-5-producing cells and their role in lung eosinophil regulation and antitumor immunity. J Immunol 2012;188:703–13.
38. Rosskopf S, Jahn-Schmid B, Schmetterer KG, Zlabinger GJ, Steinberger P. PD-1 has a unique capacity to inhibit allergen-specific human $CD4^+$ T cell responses. Sci Rep 2018;8:13543.
39. Oetjen LK, Mack MR, Feng J, Whelan TM, Niu H, Guo CJ, et al. Sensory neurons co-opt classical immune signaling pathways to mediate chronic itch. Cell 2017;171:217–28.e13.
40. Guo CJ, Grabinski NS, Liu Q. Peripheral mechanisms of itch. J Invest Dermatol 2022;142:31–41.
41. Wang F, Yang T-LB, Kim BS. The return of the mast cell: new roles in neuroimmune itch biology. J Invest Dermatol 2020;140:945–51.
42. Ruzicka T, Mihara R. Anti-Interleukin-31 receptor A antibody for atopic dermatitis. N Engl J Med 2017;376:2093.
43. Yamashita T, Akamatsu H, Tomitaka A, Ogawa Y, Sugawara N, Matsunaga K. IP-10 in atopic dermatitis. Allergy 2003;58:261.
44. Choi YA, Kim N, Jeong NH, Kwon TK, Bang JS, Jang YH, et al. Interferon-γ-inducible protein 10 augments atopic dermatitis via amplifying Th2 immune response. Allergy 2024;79:235–8.
45. Sun Z, Fourcade J, Pagliano O, Chauvin J-M, Sander C, Kirkwood JM, et al. IL10 and PD-1 cooperate to limit the activity of tumor-specific $CD8^+$ T cells. Cancer Res 2015;75:1635–44.
46. Karin N, Razon H. Chemokines beyond chemo-attraction: CXCL10 and its significant role in cancer and autoimmunity. Cytokine 2018;109:24–8.
47. Tokunaga R, Zhang W, Naseem M, Puccini A, Berger MD, Soni S, et al. CXCL9, CXCL10, CXCL11/CXCR3 axis for immune activation–a target for novel cancer therapy. Cancer Treat Rev 2018;63:40–7.
48. House IG, Savas P, Lai J, Chen AXY, Oliver AJ, Teo ZL, et al. Macrophage-derived CXCL9 and CXCL10 are required for antitumor immune responses following immune checkpoint blockade. Clin Cancer Res 2020;26:487–504.
49. Luoma AM, Suo S, Williams HL, Sharova T, Sullivan K, Manos M, et al. Molecular pathways of colon inflammation induced by cancer immunotherapy. Cell 2020;182:655–71.e22.
50. Sasson SC, Slevin SM, Cheung VTF, Nassiri I, Olsson-Brown A, Fryer E, et al. Interferon-gamma-producing $CD8^+$ tissue resident memory T cells are a targetable Hallmark of immune checkpoint inhibitor-colitis. Gastroenterology 2021;161:1229–44.e9.
51. Reschke R, Shapiro JW, Yu J, Rouhani SJ, Olson DJ, Zha Y, et al. Checkpoint blockade-induced dermatitis and colitis are dominated by tissue-resident memory T cells and Th1/Tc1 cytokines. Cancer Immunol Res 2022;10:1167–74.
52. Goldinger SM, Stieger P, Meier B, Micaletto S, Contassot E, French LE, et al. Cytotoxic cutaneous adverse drug reactions during anti-PD-1 therapy. Clin Cancer Res 2016;22:4023–9.
53. Nunez NG, Berner F, Friebel E, Unger S, Wyss N, Gomez JM, et al. Immune signatures predict development of autoimmune toxicity in patients with cancer treated with immune checkpoint inhibitors. Med 2023;4:113–29.e7.
54. Guttman-Yassky E, Irvine AD, Brunner PM, Kim BS, Boguniewicz M, Parmentier J, et al. The role of Janus kinase signaling in the pathology of atopic dermatitis. J Allergy Clin Immunol 2023;152:1394–404.
55. Mittermann I, Aichberger KJ, Bünder R, Mothes N, Renz H, Valenta R. Autoimmunity and atopic dermatitis. Curr Opin Allergy Clin Immunol 2004;4:367–71.
56. Kortekaas Krohn I, Badloe FMS, Herrmann N, Maintz L, De Vriese S, Ring J, et al. Immunoglobulin E autoantibodies in atopic dermatitis associate with type-2 comorbidities and the atopic march. Allergy 2023;78:3178–92.
57. Ten Bergen LL, Petrovic A, Aarebrot AK, Appel S. Current knowledge on autoantigens and autoantibodies in psoriasis. Scand J Immunol 2020;92:e12945.
58. Mai Y, Izumi K, Mai S, Ujiie H. The significance of preclinical anti-BP180 autoantibodies. Front Immunol 2022;13:963401.